

# Comparative Study of Physical and Magnetic Properties due to Substitution of Ni<sup>2+</sup> and Co<sup>2+</sup> in CuCo and NiCu Nanocrystalline spinel Ferrite Respectively

A.M. Tamboli<sup>1</sup>, Dr. S.M. Rathod<sup>3</sup>, Dr. Gulam Rabbani<sup>2</sup>

Associate Professor, Department of Electronic Science, Poona College, Pune, Maharashtra, India<sup>1</sup>.

Associate Professor, Department of Physics and Electronics, Maulana Azad College, Aurangabad, Maharashtra, India<sup>2</sup>.

Associate Professor, Department of Physics, Abasaheb Garware College, Pune, Maharashtra, India<sup>3</sup>.

**ABSTRACT:** Herein, the physical properties such as lattice constant  $a(\text{\AA})$ , X-ray density  $d_x(\text{gm/cm}^3)$ , bulk density ( $d_b$ ) ( $\text{gm/cm}^3$ ), porosity (%P), Particle size ( $t$ ) and magnetic properties such as Saturation magnetization [Ms(emu/gm)], Magnetic moment [Mr(emu/gm)], Coercivity [Hc(Oe)], are reported for the series  $[\text{Ni}_x\text{Cu}(\text{constant})\text{Co}_{0.8-x}\text{Fe}_2\text{O}_4]$  and  $[\text{Co}_x\text{Ni}(\text{constant})\text{Cu}_{0.8-x}\text{Fe}_2\text{O}_4]$  where constant=0.2 with  $x=0.2, 0.4$  and  $0.6$  of Nanocrystalline Spinel ferrites, synthesized by using pure metal nitrates with the help of Sol-Gel auto-combustion technique. The variation in the lattice constant  $a(\text{\AA})$ , X-ray density  $d_x(\text{gm/cm}^3)$ , bulk density ( $d_b$ ) ( $\text{gm/cm}^3$ ), porosity (%P), Particle size ( $t$ ) and variation in the Saturation magnetization [Ms(emu/gm)], Magnetic moment [Mr(emu/gm)], Coercivity [Hc(Oe)] are studied at room temperature due to the effect of substitution 'x' of Ni<sup>2+</sup> and Co<sup>2+</sup> in  $[\text{Ni}_x\text{Cu}(\text{constant})\text{Co}_{0.8-x}\text{Fe}_2\text{O}_4]$  and  $[\text{Co}_x\text{Ni}(\text{constant})\text{Cu}_{0.8-x}\text{Fe}_2\text{O}_4]$  respectively. The Nanocrystalline spinel structural of ferrite material is confirmed by XRD and Fourier Transform Infrared Spectroscopy (FT-IR). The magnetic properties are studied by using Vibrating Sample Magnetometer (VSM). The effect of substitution of Ni<sup>2+</sup> and Co<sup>2+</sup> on lattice constant  $a(\text{\AA})$ , particle size and magnetic properties of the prepared ferrite material is discussed.

**KEYWORDS :** Sol-gel auto-combustion, X-ray diffraction, FT-IR, VSM meter.

## I. INTRODUCTION

The physical and Magnetic properties of Nanocrystalline ferrite materials make them suitable for various magnetic storage applications and high frequency applications in the field of telecommunication and signal processing. Ferrites can also be used as an electromagnetic noise and wave absorber, multilayer chip inductors (MLCIs), light weight transformer core and in frequency filters. Ferrites are widely used in microwave devices such as phase splitter, circulators, insulators, and phase shifters because of their excellent magnetic properties, high resistivity and low dielectric loss. [1-2]. The general formula of ferrite is  $\text{MFe}_2\text{O}_4$  and electrical and magnetic properties of ferrites are dependent on the distribution of metal cation at tetrahedral A-site and at octahedral B-site [3-4]. Where  $\text{M}=\text{Ni}^{2+}$ ,  $\text{M}=\text{Cu}^{2+}$ ,  $\text{M}=\text{Co}^{2+}$ ,  $\text{M}=\text{Mg}^{2+}$ ,  $\text{M}=\text{Zn}^{2+}$  etc.

# International Journal of Innovative Research in Science, Engineering and Technology

(An ISO 3297: 2007 Certified Organization)

Website: [www.ijirset.com](http://www.ijirset.com)

Vol. 6, Issue 5, May 2017

## II. MATERIALS AND METHODS

### 2.1 Synthesis

Pure AR grade ferric nitrate  $[\text{Fe}(\text{NO}_3)_3 \cdot 9\text{H}_2\text{O}]$ , Copper nitrate  $[\text{Cu}(\text{NO}_3)_2 \cdot 6\text{H}_2\text{O}]$ , Nickel nitrate  $[\text{Ni}(\text{NO}_3)_2 \cdot 6\text{H}_2\text{O}]$ , Cobalt nitrate  $[\text{Co}(\text{NO}_3)_2 \cdot 6\text{H}_2\text{O}]$ , citric acid ( $\text{C}_6\text{H}_8\text{O}_7$ ), ammonium hydroxide solution ( $\text{NH}_4\text{OH}$ ) and distilled water were used to prepare the series  $[\text{Ni}_x\text{Cu}_{(\text{constant})}\text{Co}_{0.8-x}\text{Fe}_2\text{O}_4]$  and  $[\text{Co}_x\text{Ni}_{(\text{constant})}\text{Cu}_{0.8-x}\text{Fe}_2\text{O}_4]$  where constant=0.2 with  $x=0.2, 0.4$  and  $0.6$  of ferrite nanoparticles by sol-gel auto combustion synthesis technique. In this chemical process Citric acid is used as a Catalyst to boost the speed of reaction. All metal nitrates and citric acid were weighed accurately to have proper stoichiometric proportion required in the final product and all metal nitrates are dissolved in deionised water to form mixed solution. The mixed solutions of all the chemicals are stirred by using automatically rotating magnetic stirrer until the homogeneous solution is obtained. During the stirring process ammonium hydroxide solution was added drop by drop to obtain pH of liquid at 7. The mixed solution was simultaneously heated at  $100^\circ\text{C}$  for 2 hours to 4 hours such that formation of gel takes place. The transparent solution was heated at  $100^\circ\text{C}$  for 2 hours to 4 hours for removal of water and solution turns into a viscous brown gel. The temperature of the gel was further increased up to  $140^\circ\text{C}$  to  $180^\circ\text{C}$  such that combustion of the gel takes place and fine powder of  $[\text{Ni}_x\text{Cu}_{(\text{constant})}\text{Co}_{0.8-x}\text{Fe}_2\text{O}_4]$  and  $[\text{Co}_x\text{Ni}_{(\text{constant})}\text{Cu}_{0.8-x}\text{Fe}_2\text{O}_4]$  ferrite nanoparticles are obtained.

The powder was dried and annealed at  $400^\circ\text{C}$  for 4h in furnace having super kanthal ( $\text{MoSi}_2$ ) heating elements and alumina insulation boards as chamber walls. Total six samples of ferrite materials are prepared out of that three samples of ferrite materials are prepared for  $[\text{Ni}_x\text{Cu}_{(\text{constant})}\text{Co}_{0.8-x}\text{Fe}_2\text{O}_4]$  and three for  $[\text{Co}_x\text{Ni}_{(\text{constant})}\text{Cu}_{0.8-x}\text{Fe}_2\text{O}_4]$  for constant=0.2 with  $x=0.2, 0.4$  and  $0.6$ . Detail composition of all samples all six samples are represented by symbol A, B, C, D, E, A is shown in Table. No.1.

### 2.2 Characterization of Lattice Constant and Particle Size.

The phase analysis and gross structural analysis is done by using X-ray diffractometer ( $\text{Cu K}\alpha_1$  radiation= $1.5418 \text{ \AA}$ ) and confirmation of single phase spinel structure is done. The average particle size of prepared powder has been calculated using Scherrer formula

$$t = 0.9 \lambda / \beta \cos \theta \quad \text{-----} \quad (1)$$

Where;  $\lambda$  = Wave length of X-rays.

t = Particle size.

$\theta$  = Bragg's angle.

$\beta$  = Full Width Half Maxima of the recorded peak  $\theta$  and it is corrected for instrumental broadening.

The lattice parameter (a) is calculated from X-ray diffraction data by using formula

$$1/d^2 = 1/a^2 * (h^2 + k^2 + l^2) \quad \text{-----} \quad (2)$$

Using the XRD data, the interplaner spacing 'd' values for all the reflections were determined using Bragg's law. It is observed that due to the concentration of  $\text{Ni}^{2+}$  ions in place of  $\text{Co}^{2+}$  ions the Bragg's angle shifts towards higher angle and thereby interplaner spacing 'd' values decreases [1-3]. The lattice constant is found to decrease with increase in  $\text{Ni}^{2+}$  concentration x. The variations in lattice constant as a function of Nickel concentration x can be understood on the basis of the ionic radius of the substituted cations. Since the ionic radius of  $\text{Ni}^{2+}$  ions ( $0.69 \text{ \AA}$ ) is less than that of  $\text{Co}^{2+}$  ions ( $0.745 \text{ \AA}$ ), the substitution is expected to decrease the lattice constant with increase in nickel concentration x [4-5]. When the smaller nickel ion enters, the lattice unit cell expands while preserving overall symmetry this is true as long as the lattice constant decreases with substituent concentration x.

# International Journal of Innovative Research in Science, Engineering and Technology

(An ISO 3297: 2007 Certified Organization)

Website: [www.ijirset.com](http://www.ijirset.com)

Vol. 6, Issue 5, May 2017

The values of lattice constant obtained from XRD data for varying nickel concentration  $x$  are given in Table 2. It can be seen from Table 2 that, the lattice constant decreases linearly with nickel concentration  $x$  and obeys Vegard's law [6-9]. The values of particle size obtained from Scherrer formula are given in Table 3. It can be seen from Table 3 that the particle size decreases with increase in  $\text{Ni}^{2+}$  substitution  $x$ .

It is observed that due to the concentration of  $\text{Co}^{2+}$  ions in place of  $\text{Cu}^{2+}$  ions the Bragg's angle shifts towards lower angle and thereby interplaner spacing 'd' values increases. The lattice constant is found to increase with increase in  $\text{Co}^{2+}$  concentration  $x$ . The variations in lattice constant as a function of Cobalt concentration  $x$  can be understood on the basis of the ionic radius of the substituted cations. Since the ionic radius of  $\text{Co}^{2+}$  ions ( $0.745\text{\AA}$ ) is greater than that of  $\text{Cu}^{2+}$  ions ( $0.73\text{\AA}$ ), the substitution is expected to increase the lattice constant with increase in Cobalt concentration  $x$ . When the larger Cobalt ions enters, the lattice unit cell expands while preserving overall symmetry this is true as long as the lattice constant increases with substituent concentration of Cobalt.

The values of lattice constant obtained from XRD data for varying Cobalt concentration  $x$  are given in below Table 4. It can be seen from Table 4 that the lattice constant increases with Cobalt concentration  $x$  and obeys Vegard's law [10-12]. The values of particle size for varying Cobalt concentration  $x$  is obtained from Scherrer formula and it is given in Table 5. It can be seen from Table 5 that the particle size increases with increase in  $\text{Co}^{2+}$  substitution  $x$ .

## 2.3 Characterization of Saturation magnetization [ $M_s$ (emu/gm)] and Coercivity [ $H_c$ (Oe)].

With increasing  $\text{Ni}^{2+}$  density 'x' in  $[(\text{Ni}_x \text{Cu}_{(\text{constant})} \text{Co}_{0.8-x})\text{Fe}_2\text{O}_4]$  for constant=0.2 with  $x=0.2, 0.4$  and  $0.6$ , Saturation magnetization [ $M_s$  (emu/gm)] of ferrite material increases and Coercivity [ $H_c$ (Oe)] decreases for three materials namely A, B and C. The total magnetization of the Spinel ferrites comes from the difference in the magnetization of B-sites and A-sites and it is also known that the octahedral (B) site has larger magnetic moment than the tetrahedral (A) site [13-20]. Table 6 shows the Values of [ $M_s$  (emu/gm)] and [ $H_c$ (Oe)]. Fig. 6 indicates variation in [ $M_s$  (emu/gm)] with substitution  $x$  of  $\text{Ni}^{2+}$ , Fig. 7 indicates variation in [ $H_c$ (Oe)] with substitution  $x$  of  $\text{Ni}^{2+}$  and Fig. 8 shows the Hysteresis loop of ferrite samples of A, B and C.

With increasing  $\text{Co}^{2+}$  density 'x' in  $[\text{Co}_x (\text{Ni}_{(\text{constant})} \text{Cu}_{0.8-x})\text{Fe}_2\text{O}_4]$  for constant=0.2 with  $x=0.2, 0.4$  and  $0.6$ , Saturation Magnetization [ $M_s$  (emu/gm)], Magnetic moment [ $M_r$ (emu/gm)] and Coercivity [ $H_c$ (Oe)] of ferrite material increases for three materials namely D, E and A. Table 7 shows the Values of [ $M_s$  (emu/gm)] and [ $H_c$ (Oe)]. Fig. 9 indicates variation in [ $M_s$  (emu/gm)] with substitution  $x$  of  $\text{Co}^{2+}$ , Fig. 10 indicates variation in [ $H_c$ (Oe)] with substitution  $x$  of  $\text{Co}^{2+}$  and Fig. 11 shows the Hysteresis loop of ferrite samples of D, E and A.

The FTIR spectroscopy confirms the single phase nature of the prepared sample. The peak  $536.114 \text{ cm}^{-1}$  gives the confirmation of  $\text{Fe}_2\text{O}_4$ .

## III. RESULTS AND DISCUSSIONS

### 3.1: Structural and Magnetic properties analysis.

The XRD pattern of as-synthesized ferrite material of  $[\text{Ni}_x \text{Cu}_{(\text{constant})} \text{Co}_{0.8-x} \text{Fe}_2\text{O}_4]$  is shown in Fig.1. The highest intensity peaks in all three specimens are observed at (311). The average grain (crystallite) size for all the composites is calculated using Scherer's formula with respect to the high intense peak plane (311) and Lattices Constant  $a$  ( $\text{\AA}$ ) is calculated by using the formula  $1/d^2 = 1/a^2 * (h^2 + k^2 + l^2)$ . It is observed that due to the concentration of  $\text{Ni}^{2+}$  ions in place of  $\text{Co}^{2+}$  ions the Bragg's angle shifts towards higher angle and thereby interplaner spacing 'd' values decreases. The lattice constant is found to decrease with increase in Nickel ( $\text{Ni}^{2+}$ ) concentration  $x$ . The lattice constant is found to decrease with increase in  $\text{Ni}^{2+}$  concentration  $x$ .

With increasing  $\text{Ni}^{2+}$  density 'x' in  $[(\text{Ni}_x \text{Cu}_{(\text{constant})} \text{Co}_{0.8-x})\text{Fe}_2\text{O}_4]$  Saturation magnetization [ $M_s$  (emu/gm)] of ferrite material increases and Coercivity [ $H_c$ (Oe)] decreases for three materials namely A, B and C.

# International Journal of Innovative Research in Science, Engineering and Technology

(An ISO 3297: 2007 Certified Organization)

Website: [www.ijirset.com](http://www.ijirset.com)

Vol. 6, Issue 5, May 2017

It is observed that due to the increase concentration of  $\text{Co}^{2+}$  ions in Ni Cu the Bragg's angle shifts towards lower angle and thereby interplaner spacing's (d) values increases. The XRD pattern contains no secondary peaks and it gives the confirmation about pure spinal structure of sample.

When the larger Cobalt ions enters, the lattice unit cell expands while preserving overall symmetry this is true as long as the lattice constant increases with substituent concentration of Cobalt. It can be seen from Table 1.that, the lattice constant increases with increase of Cobalt ( $\text{Co}^{2+}$ ) concentration x.

With increasing  $\text{Co}^{2+}$  density 'x' in  $[\text{Co}_x (\text{Ni}_{(\text{constant})} \text{Cu}_{0.8-x}) \text{Fe}_2\text{O}_4]$ , Saturation Magnetization [Ms (emu/gm)] and Coercivity [Hc(Oe)] of ferrite material increases for three materials namely D, E and A.

The FTIR spectroscopy confirms the single phase nature of the prepared sample. The peak  $536.114 \text{ cm}^{-1}$  gives the confirmation of  $\text{Fe}_2\text{O}_4$ .

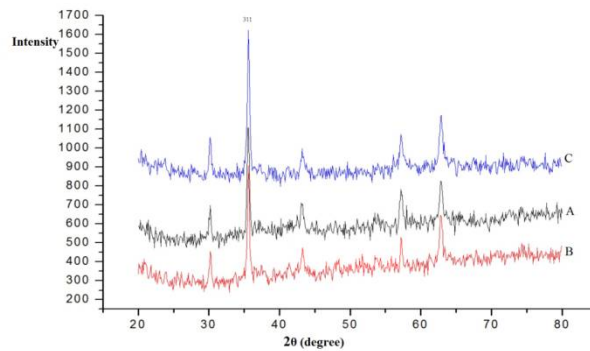


Fig. 1. XRD of Ferrite samples A, B and C

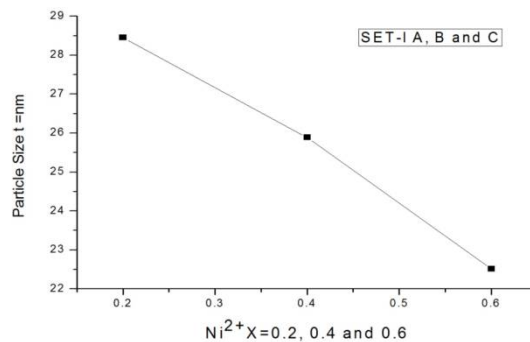


Fig. 2. Particle size (t) versus  $\text{Ni}^{2+}$  substitution x=0.2, 0.4 and 0.6.

# International Journal of Innovative Research in Science, Engineering and Technology

(An ISO 3297: 2007 Certified Organization)

Website: [www.ijirset.com](http://www.ijirset.com)

Vol. 6, Issue 5, May 2017

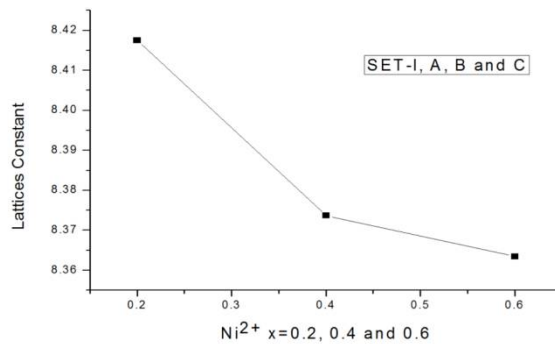


Fig. 3. Lattice Constant Verses Ni<sup>2+</sup> substitution x=0.2, 0.4 and 0.6

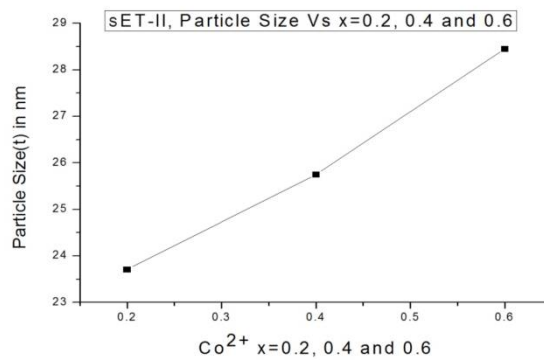


Fig. 4. Particle size (t) verses Co<sup>2+</sup> substitution x in SET-II (D, E, A).

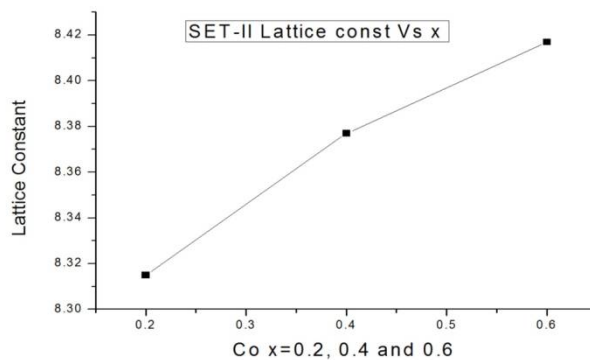


Fig. 5. Lattices Constant verses Co<sup>2+</sup> substitution x in SET-II (D, E, A).

# International Journal of Innovative Research in Science, Engineering and Technology

(An ISO 3297: 2007 Certified Organization)

Website: [www.ijirset.com](http://www.ijirset.com)

Vol. 6, Issue 5, May 2017

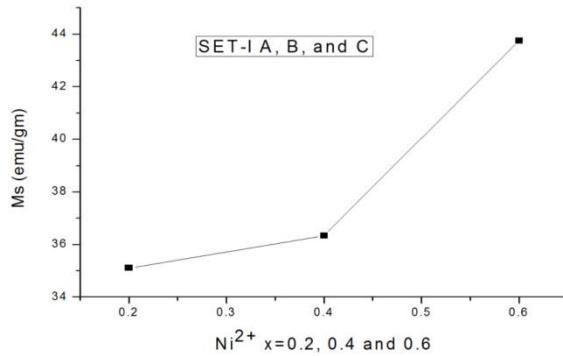


Fig. 6. Ms (emu/gm) Verses Ni<sup>2+</sup> substitution x=0.2, 0.4 and 0.6.

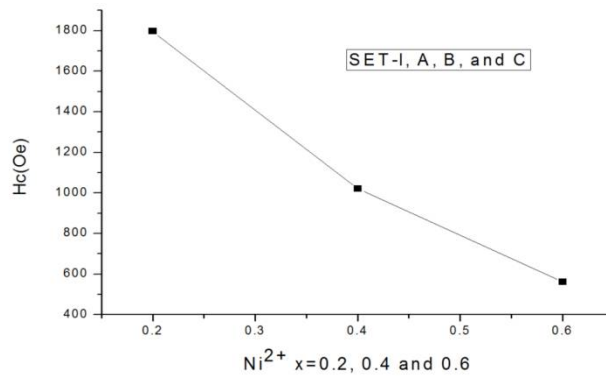


Fig. 7. Hc(Oe) Verses Ni<sup>2+</sup> substitution x=0.2, 0.4 and 0.6.

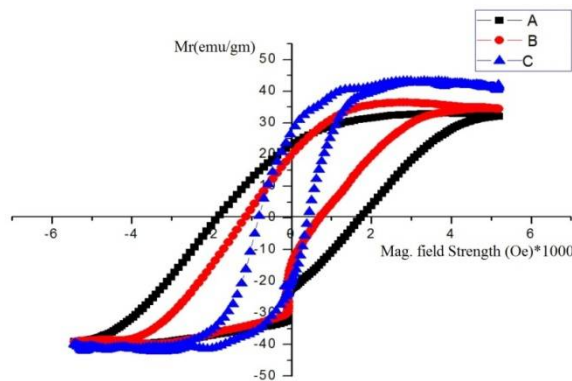


Fig. 8. Hysteresis Loop of three ferrite materials in SET-I (A,B,C).

# International Journal of Innovative Research in Science, Engineering and Technology

(An ISO 3297: 2007 Certified Organization)

Website: [www.ijirset.com](http://www.ijirset.com)

Vol. 6, Issue 5, May 2017

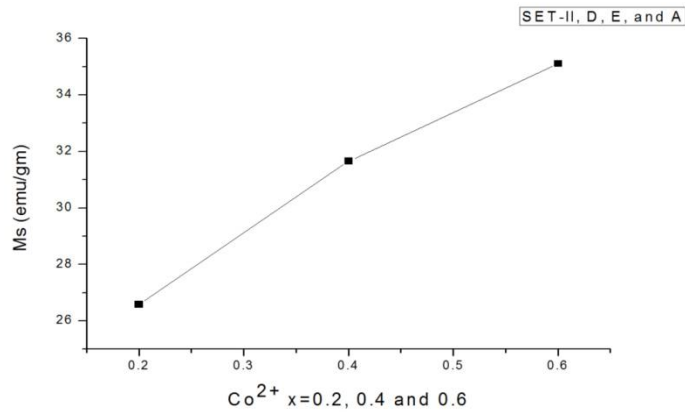


Fig. 9. Ms (emu/gm) Verses Co<sup>2+</sup> substitution x=0.2, 0.4 and 0.6.

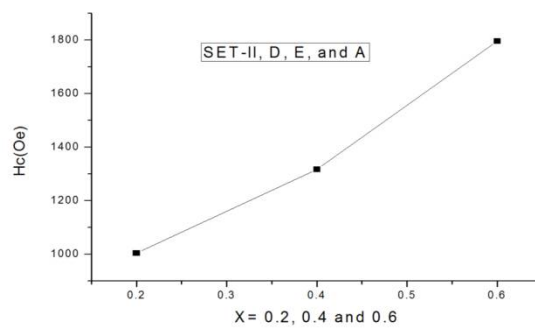


Fig. 10. Hc(Oe) Verses Co<sup>2+</sup> substitution x=0.2, 0.4 and 0.6.

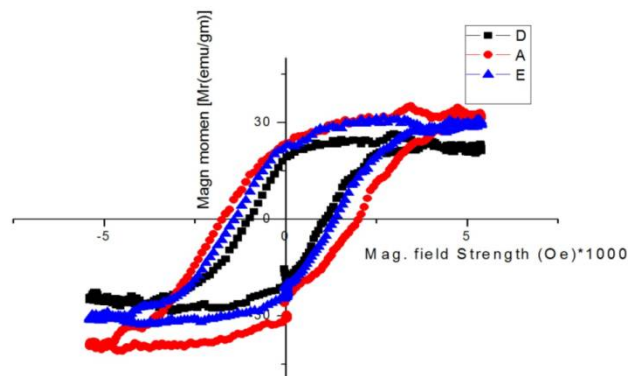


Fig. 11. Hysteresis Loop of three ferrite materials in SET-II (D, E, A).

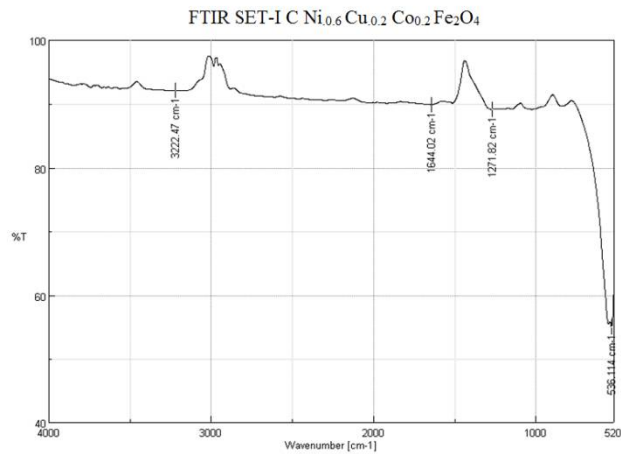


Fig. 12. FTIR graph for SET-I (C)  $[(Ni_{0.6}Cu_{0.2}Co_{0.2})Fe_2O_4]$

Table 1.  
Composition of Samples A, B, C, D, E, and A.

SET	Label	Ferrite Material
SET-I	A	$[(Ni_{0.2}Cu_{0.2}Co_{0.6})Fe_2O_4]$
	B	$[(Ni_{0.4}Cu_{0.2}Co_{0.4})Fe_2O_4]$
	C	$[(Ni_{0.6}Cu_{0.2}Co_{0.2})Fe_2O_4]$
SET-II	D	$[(Co_{0.2}Ni_{1.0}Cu_{0.6})Fe_2O_4]$
	E	$[(Co_{0.4}Ni_{1.0}Cu_{0.4})Fe_2O_4]$
	A	$[(Co_{0.6}Ni_{1.0}Cu_{0.2})Fe_2O_4]$

Table 2.  
Variation of Particle size (t) and lattice constant a(Å) for SET-I(A,B,C).

Ferrite Sample and X	Particle Size t (nm)	Lattices Constant (Å)
(A) for X=0.2	28.45	8.417
(B) for X=0.4	25.89	8.374
(C) for X=0.6	22.52	8.364

Table 3.  
Variation of Particle size (t) and Lattices Constant (Å) for SET-II (D, E, A).

Ferrite Sample and X	Particle Size t (nm)	Lattices Constant (Å)
(D) for X=0.2	23.71	8.315
(E) for X=0.4	25.75	8.377
(A) for X=0.6	28.45	8.417



## International Journal of Innovative Research in Science, Engineering and Technology

(An ISO 3297: 2007 Certified Organization)

Website: [www.ijirset.com](http://www.ijirset.com)

Vol. 6, Issue 5, May 2017

Table 4.  
Comparison of VSM data for SET-I, A, B and C.

SAMPLE	Hc(Oe)	Ms (emu/gm)
(A) Ni <sub>0.2</sub> Cu <sub>0.2</sub> Co <sub>0.6</sub> Fe <sub>2</sub> O <sub>4</sub>	1796.6049	035.1130
(B) Ni <sub>0.4</sub> Cu <sub>0.2</sub> Co <sub>0.4</sub> Fe <sub>2</sub> O <sub>4</sub>	1022.1605	036.3335
(C) Ni <sub>0.6</sub> Cu <sub>0.2</sub> Co <sub>0.2</sub> Fe <sub>2</sub> O <sub>4</sub>	560.8642	043.7550

Table 5.  
Comparison of VSM data for SET-II, D, E and A.

SAMPLE	Hc(Oe)	Ms (emu/gm)
(D) Ni <sub>0.2</sub> Cu <sub>0.6</sub> Co <sub>0.2</sub> Fe <sub>2</sub> O <sub>4</sub>	1004.9383	026.5841
(E) Ni <sub>0.2</sub> Cu <sub>0.4</sub> Co <sub>0.4</sub> Fe <sub>2</sub> O <sub>4</sub>	1317.9630	031.6586
(A) Ni <sub>0.2</sub> Cu <sub>0.2</sub> Co <sub>0.6</sub> Fe <sub>2</sub> O <sub>4</sub>	1796.6049	035.1130

### IV. CONCLUSION

We have successfully implemented Sol Gel Auto combustion method and successfully fabricated the Nanocrystalline Ferrite materials namely [(Ni<sub>0.2</sub>Cu<sub>0.2</sub>Co<sub>0.6</sub>)Fe<sub>2</sub>O<sub>4</sub>], [(Ni<sub>0.4</sub>Cu<sub>0.2</sub>Co<sub>0.4</sub>)Fe<sub>2</sub>O<sub>4</sub>], [(Ni<sub>0.6</sub>Cu<sub>0.2</sub>Co<sub>0.2</sub>)Fe<sub>2</sub>O<sub>4</sub>], [(Co<sub>0.2</sub>Ni<sub>0.2</sub>Cu<sub>0.6</sub>)Fe<sub>2</sub>O<sub>4</sub>], [(Co<sub>0.4</sub>Ni<sub>0.2</sub>Cu<sub>0.4</sub>)Fe<sub>2</sub>O<sub>4</sub>] with good magnetic properties.

### REFERENCES

- [1] C. G. Whinfrey, D. W. Eckort and A. Tauber, *J. Am. Chem. Soc.* 53, pp 272-282, 1982.
- [2] C. Caizer, M. Stefanescu, *J. Phys. D. Appl. Phys.* 35 pp 30-35, 2002.
- [3] M.A. Ahmed, S.F. Mansour, M. Afifi, *J. Magn. Magn. Mater.* 324 pp 4-10, 2012.
- [4] P.S. Aghav, V.N. Dhage, M.L. Mane, D.R. Shengule, R.G. Dorik, K.M. Jadhav, *Physica B: Cond. Matter.* 406 pp 43-50, 2011.
- [5] J. Jing, L. Liangchao, X. Feng, *J. Rare Earths* 25 pp 79-81, 2007.
- [6] S. Sun, C.B. Murray, D. Weller, L. Folks, A. Moser, *Science* 287, 198-199, 2000.
- [7] I.H. Gul, W. Ahmed, A. Maqsood, *J. Magn. Magn. Mater.* 320 pp 270-275, 2008.
- [8] D.K. Kim, Y. Zhang, W. Voit, K.V. Rao, M. Mohammed, *J. Magn. Magn. Mater.* 225, pp 30-34, 2001.
- [9] M. R. Barati, *J Sol-Gel Sci Technol* 52 pp 171-177, 2009.
- [10] A.T. Raghavendar, Damir Pajic, Kreso Zadro, Tomislav Milekovic, P. Vekateshwar Rao, K.M. Jadhav, D. Ravinder, *J. Magn. Magn. Mater.* 3 pp 204-210, 2007.
- [11] C. G. Whinfrey, D. W. Eckort and A. Tauber, *J. Am. Chem. Soc.* 53, pp 272-282, 1982.
- [12] C. Caizer, M. Stefanescu, *J. Phys. D. Appl. Phys.* 35, pp 30-35, 2002.
- [13] M.A. Ahmed, S.F. Mansour, M. Afifi, *J. Magn. Magn. Mater.* 324, pp 4-10, 2012.
- [14] P.S. Aghav, V.N. Dhage, M.L. Mane, D.R. Shengule, R.G. Dorik, K.M. Jadhav, *Physica B: Cond. Matter.* Pp 406- 430, 2011
- [15] K.W. Wagner, *Ann. Phys.* 40, pp 817-820, 1913.
- [16] I.T. Rabinkin, Z.I. Novikova, *Ferrites, Izv Acad. Nauk USSR, Minsk*, 1960.
- [17] J.C. Maxwell, *Electricity and Magnetism, vol. 1, Oxford University Press, New York* (1973), p. 1.
- [18] M. Penchal Reddy, W. Madhuri, N. Ramamanoher Reddy, K.V. Siva Kumar, V.R.K. Murthy, R. Ramakrishna Reddy, Influence of copper substitution on magnetic and electrical properties of MgCuZn ferrite prepared by microwave sintering method, *Mater. Sci. Eng. C* 30, pp 1094-1099, 2010.
- [19] J. Azadmanjiri, H.K. Salehani, M.R. Barati, F. Farzan, Preparation and electromagnetic properties of Ni<sub>x</sub>Cu<sub>y</sub>Fe<sub>2</sub>O<sub>4</sub> nanoparticle ferrites by sol-gel auto-combustion method, *Mater. Lett.* 61, pp 84-87, 2007.
- [20] J. Du, Z. Liu, W. Wu, Z. Li, B. Han, Y. Huang, Preparation of single-crystal copper ferrite nanorods and nanodisks, *Mater. Res. Bull.* 40 pp 928-935, 2005.